

A reanalysis of the $k^3\Pi$ state of CO

Giel Berden, Rienk T. Jongma, Dorien van der Zande, and Gerard Meijer

Department of Molecular and Laser Physics, University of Nijmegen, Toernooiveld, 6525 ED Nijmegen, The Netherlands

(Received 22 July 1997; accepted 21 August 1997)

The $k^3\Pi$ state of the CO molecule is investigated in the region between 91 000 and 97 000 cm^{-1} via 1+1 resonance enhanced multiphoton ionization spectroscopy on CO molecules prepared in a single quantum level of the $a^3\Pi(v=1)$ state. A new vibronic band is found which is at lower energy than the vibrational ground state reported in the literature, leading to a reassignment of the vibrational numbering of the $k^3\Pi$ state. The rotationally resolved spectra of the $k^3\Pi(v=0-6) \leftarrow a^3\Pi(v=1, J=1, \Omega=1)$ of ^{12}CO and ^{13}CO have been observed and analyzed, confirming the new vibrational labeling and providing a full set of molecular constants of the $k^3\Pi$ valence state. © 1997 American Institute of Physics. [S0021-9606(97)02644-5]

I. INTRODUCTION

The $k^3\Pi$ state of CO in the 90 000–98 000 cm^{-1} range has first been observed by Mazeau *et al.*¹ by electron impact spectroscopy just over 20 years ago. They observed a somewhat irregular vibrational progression of five peaks (named ‘‘a–e’’ bands) followed by a ‘‘plateau,’’ indicating a dissociation continuum, and assigned these features to a transition into a $^3\Pi$ valence state. A bound valence triplet state was already calculated to exist in this region by O’Neil and Schaefer (their $^3\Pi$ II state).²

After populating the $a^3\Pi$ state via electron beam excitation, Wan and Langhoff³ have measured triplet–triplet transitions starting from the $a^3\Pi$ state. Their reported spectrum contains a progression of five bands. The two bands with the highest energy correspond with the ‘‘a’’ and ‘‘b’’ bands of Mazeau *et al.*¹ Based on partially rotationally resolved spectra, they assigned these five bands to the $v=0-4$ of the $j^3\Sigma^+$ state (the ‘‘a–e’’ bands of Mazeau *et al.* correspond then to the $v=3-7$ bands).

In a study of indirect predissociations of the $E^1\Pi(v=1)$ state of CO, Baker *et al.*⁴ showed that the partially resolved spectra of Wan and Langhoff³ are much better simulated by a $^3\Pi \leftarrow ^3\Pi$ transition than by a $^3\Sigma^+ \leftarrow ^3\Pi$ transition, thus confirming the original assignment of Mazeau *et al.* This valence triplet state was then labeled by Baker *et al.*⁴ as the k state. In order to confirm the symmetry character of the k state and to obtain its molecular constants, Baker and Launay⁵ recorded the high resolution vacuum ultraviolet (VUV) spectrum of CO in the 90 000–98 000 cm^{-1} range. They observed the $k^3\Pi(v=2,3,5) \leftarrow X^1\Sigma^+(v=0)$ absorption bands and performed a rotational analysis of these bands. The $v=2$ band lies on top of the recently discovered diffuse $B^1\Sigma^+(v=3) \leftarrow X^1\Sigma^+(v=0)$ band.⁶ For the $k^3\Pi(v=5) \leftarrow X^1\Sigma^+(v=0)$ band, only a few rotational lines were observed due to the overlap with the more intense $E^1\Pi(v=1) \leftarrow X^1\Sigma^+(v=0)$ transition.⁵ The $k^3\Pi(v=0) \leftarrow X^1\Sigma^+(v=0)$ transition, which is partially overlapped with the (more intense) $B^1\Sigma^+(v=2) \leftarrow X^1\Sigma^+(v=0)$ band, has been observed and analyzed by Baker.⁷ At the same time, Mellinger and Vidal⁸ observed the rotationally resolved spectrum of the

$k^3\Pi(v=1)$ state in a double-resonance experiment via the $a'^3\Sigma^+(v=14)$ intermediate state.

It is suggested that the $k^3\Pi$ state is responsible for perturbations in the rotational structure of the $c^3\Pi(v=0)$ state^{4,9} although no evidence is found for this yet. Baker has shown that the $k^3\Pi$ state is responsible for the localized perturbations in the $E^1\Pi(v=0,1)$ ^{4,5} and $B^1\Sigma^+(v=2)$ ⁷ states. For example, the $k^3\Pi_2(v=3)$ spin-orbit component causes the indirect predissociation at $J=31$ in the $E^1\Pi(v=0)$ state, while the $k^3\Pi_0(v=5)$ spin-orbit component causes the indirect predissociations at $J=7$ in the $E^1\Pi(v=1)$ state.⁵ The latter localized indirect predissociations have also been observed for the $J=7$ rotational level of different isotopes of CO,⁴ which is rather surprising for a localized perturbation. The accidental predissociations in the $E^1\Pi(v=0,1)$ states were recently investigated in detail by Cacciani *et al.*¹⁰ They developed a quantitative description of the perturbations based on a spin-orbit interaction between the $E^1\Pi$ state and the $^3\Pi_1$ component of the $k^3\Pi$ state.

In summary, up to now five vibronic bands of the $k^3\Pi$ state have been observed at rotational resolution, i.e., the $v=0,1,2,3$, and 5, and in addition $v=4,6$ and 7 have been observed at vibrational resolution (electron impact spectroscopy¹). A disadvantage of the spectroscopic studies in which CO molecules are excited from the electronic ground state, is the observation of intense singlet–singlet transitions which might overlap the spin-forbidden $k^3\Pi \leftarrow X^1\Sigma^+$ transition.^{1,5,7} Populating a triplet state and performing a spectroscopic study starting from this state, can overcome this problem.^{3,8,11}

In a resonant enhanced multiphoton ionization (REMPI) study of a molecular beam of $a^3\Pi_1(v=0, J=1)$ CO molecules we have found a spectrum with a rotational structure which matches the $k^3\Pi$ state very well, but is lower in energy than the reported $v=0$ level of the $k^3\Pi$ state. The energy difference between this band and the $v=0$ band is 811 cm^{-1} , in good agreement with the reported value of $\omega_e=836 \text{ cm}^{-1}$.⁷ We therefore have to conclude that the vibrational assignment of the $k^3\Pi$ state found in the literature is not correct. In order to determine the correct vibrational assignment, and to obtain more information about the vibrational

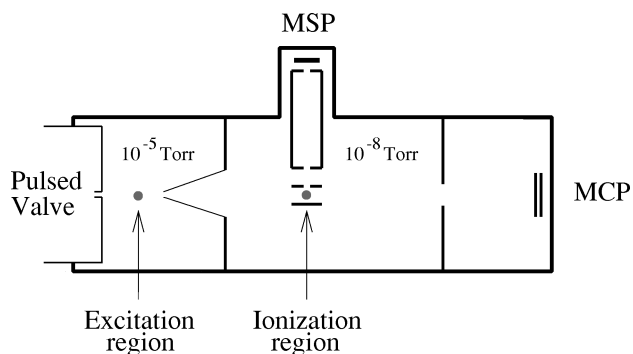


FIG. 1. Schematic overview of the vacuum machine, composed of three differentially pumped chambers. The pulsed valve releases short pulses of CO diluted in argon. Metastable $a^3\Pi(v=1)$ CO molecules are prepared via pulsed laser excitation around 199 nm of jet-cooled ground state CO molecules and enter the ionization chamber through a skimmer. In this chamber a compact Wiley–McLaren type time-of-flight mass spectrometer is mounted, and REMPI spectroscopy is performed on the metastable CO molecules with a second laser. Downstream from the mass spectrometer the amount of metastable CO molecules is directly monitored by a MCP detector.

and rotational structure of the $k^3\Pi$ state, we (re)measured the rotational spectra of as many vibronic bands of ^{12}CO and ^{13}CO as possible. Comparing the results of both isotopes leads to an unambiguous vibrational labeling: every vibrational quantum number in this introduction, and therefore every vibrational quantum number of the $k^3\Pi$ state that appeared in the literature up to now, has to be raised by 1. In the remaining part of this paper, this new vibrational labeling will be used.

II. EXPERIMENT

Metastable $a^3\Pi(v=1)$ CO molecules are formed by laser excitation of jet-cooled CO. These metastable molecules are ionized via (1+1)-REMPI with a second laser that is resonant with ro-vibrational transitions in the $k^3\Pi \leftarrow a^3\Pi(v=1)$ band of CO.

The vacuum system is composed of three differentially pumped stainless steel vacuum chambers (see Figure 1). In the first chamber, the source chamber, a pulsed valve (R.M. Jordan Co.) operating on the magnetic repulsion principle is mounted. The valve has a 0.35-mm-diam orifice and delivers gas pulses of typically 30 μs duration at a repetition frequency of 10 Hz. A mixture of 20% CO (^{12}CO or ^{13}CO) in argon at a total backing gas pressure of 2 atm is used for the supersonic expansion. About 2 cm downstream from the nozzle the jet-cooled ground state CO molecules are excited to the $J=1$ rotational level of the metastable $a^3\Pi(v=1)$ state by pulsed 199 nm laser radiation. The lifetime of this quantum level is 3.6 ms.¹²

Narrow band laser light is produced with an argon-ion laser (Spectra Physics 2017) pumped cw-ring dye laser system (Spectra Physics 380), running on Rhodamine 6G, that produces 300 mW of 597 nm laser light in a 1 MHz bandwidth. The output of the cw laser is amplified in a Nd:YAG laser (Spectra Physics GCR-3) pumped pulsed dye amplified system (Lambda Physik LPD 3000) running on Rhodamine

640. The pulsed laser radiation around 597 nm is frequency-tripled in the combination of a potassium dihydrogen phosphate (KDP) and a $\beta\text{-BaB}_2\text{O}_4$ (BBO) crystal. The 199 nm laser light that is obtained (0.5 mJ in a 150 MHz bandwidth), is separated from the fundamental and second harmonic using a number of 45° mirrors for 199 nm laser light ($R > 98\%$, Laseroptik GmbH). The favourable spectral brightness of this laser system, as compared to normal pulsed dye lasers, allows efficient pumping on the $a^3\Pi \leftarrow X^1\Sigma^+$ transition. Preparation of the $a^3\Pi(v=1)$ state at 199 nm has been chosen instead of preparation of the $a^3\Pi(v=0)$ state at 206 nm for experimental reasons; the ring dye laser operates more stably on 597 nm (top of the gain curve of Rhodamine 6G) than at 618 nm (mixture of Rhodamine 6G and DCM). Although not presented in this paper, the $k^3\Pi(v=0) \leftarrow a^3\Pi(v=0)$ spectrum has been measured as well.

After passing the excitation region, the molecular beam is collimated by a 0.8-mm-diam skimmer located 4 cm away from the nozzle, and enters the differentially pumped REMPI chamber. In this chamber a small Wiley–McLaren type time-of-flight (TOF) mass spectrometer¹³ is mounted 7.5 cm downstream from the excitation region. The (gridless) extraction electrodes have a diameter of 17.5 mm and are equally spaced at a distance of 6 mm. The grounded field free flight tube has a length of 10 cm. At the end of the flight tube the ions are detected on a micro-sphere plate (MSP) detector (El-Mul). Only the upper electrode of the flight tube is equipped with a grid, to shield for electric stray fields caused by the voltages applied to the MSP detector. The mass resolution, defined by the ratio $m/\Delta m$ in which Δm is the full width at half maximum, of this compact mass spectrometer is determined to be 33. Ionization from the metastable state in CO is performed between the lower two extraction plates via (1+1)-REMPI with a second laser that is resonant with ro-vibrational transitions in the $k^3\Pi \leftarrow a^3\Pi$ band of CO. The laser used for excitation and ionization of metastable CO molecules is a Nd:YAG pumped pulsed dye laser system (Spectra Physics GCR-3/PDL-3 combination) running on coumarine dyes. The output of this laser is frequency-doubled in a BBO crystal, producing a few mJ of ultraviolet (UV) radiation (220–250 nm) with a bandwidth of 0.15 cm^{-1} . A small fraction of the fundamental laser output is used for calibrating the frequency by recording the absorption spectrum of Te_2 ¹⁴ simultaneously with the REMPI spectrum of CO.

After passage through the mass spectrometer, the molecular beam enters the third chamber where it impinges upon a 25-mm-diam micro-channel plate (MCP) detector (R.M. Jordan Co.) that is used for selective detection of the metastable CO molecules. The signal from the MCP detector is used to optimize alignment and frequency of the 199 nm excitation laser, and is used as a reference for the number of metastable molecules present in the molecular beam. All chambers are pumped by turbomolecular pumping systems, yielding background pressures, under operating conditions, of $1.5 \cdot 10^{-5}$ Torr in the source chamber, $2.0 \cdot 10^{-8}$ Torr in the REMPI chamber, and $2.0 \cdot 10^{-10}$ Torr in the MCP chamber.

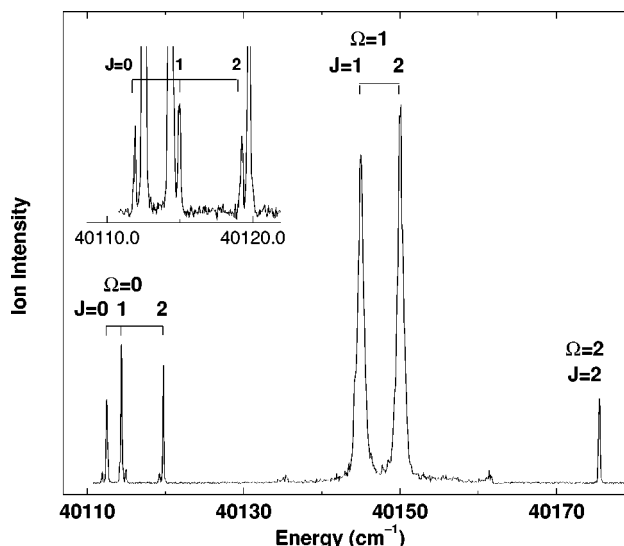


FIG. 2. (1+1)-REMPI spectrum of the $k^3\Pi(v=0) \leftarrow a^3\Pi(v=1, J=1, \Omega=1)$ band of ^{12}CO . The spectrum consists of only six lines since a single quantum state ($J=1, \Omega=1, +$ parity) in the $a^3\Pi$ state has been prepared. These lines can be assigned to, in order of increasing frequency, the $^oP_{12}(1)$, $^pQ_{12}(1)$, $^oR_{12}(1)$, $^oQ_{22}(1)$, $^pR_{22}(1)$, and the $^sR_{32}(1)$ transition. In the figure, only the quantum numbers in the $k^3\Pi$ state are given. The transitions to the $\Omega=1$ levels are saturated. Weak lines are observed close to the $\Omega=0$ lines, and are shown more clearly in the inset. They can be assigned as transitions to the $J=0,1,2 \Omega=0$ levels starting from the $J=1, \Omega=1, -$ parity level in the $a^3\Pi(v=1)$ state, which is populated via remaining collisions in and after the excitation region.

The REMPI signal recorded by the MSP and the Te_2 absorption signal recorded by a photodiode are fed into a digital oscilloscope with a 10 bit vertical resolution (LeCroy 9430). The signals are digitized, summed over typically 25 laser shots, and then read out by a computer (486PC) via a GPIB interface (National Instruments). The signals in preset time gates are averaged and recorded after subtraction of the baseline. The energy of the ionization laser and the amount of metastable CO molecules in the beam, the latter monitored via the MCP detector, are recorded simultaneously with the ion signal. Both signals are averaged on gated integrator/boxcar averagers [Stanford Research Systems (SRS) 250] because of the presence of only two channels on the oscilloscope. The averaged outputs of the boxcars are digitized by a 13 bit digitizer (SRS 245) and read into the computer together with the oscilloscope signals. Thus recorded REMPI spectra can be corrected for intensity fluctuations in the beam of metastable CO molecules and for fluctuations in the energy of the ionization laser. Synchronization of pulsed valve, lasers and oscilloscope is achieved with a delay generator (SRS DG535).

III. RESULTS

Figure 2 shows a typical (1+1)-REMPI spectrum of a vibronic band of the $k^3\Pi \leftarrow a^3\Pi(v=1)$ system of CO after preparation of the $J=1, \Omega=1, +$ parity level in the $a^3\Pi(v=1)$ state. Preparation is performed via the $Q_2(1)$ transition. The spectrum shown here is that of the $k^3\Pi(v=0) \leftarrow a^3\Pi(v=1)$ band of ^{12}CO , but the rotational structure of

the other bands of both ^{12}CO and ^{13}CO are basically the same. Since all transitions start from a well defined single quantum level, the analysis of this spectrum is straightforward. The selection rules are $\Delta\Omega=0, \pm 1$, $\Delta J=0, \pm 1$, and $+\leftrightarrow -$. The two strongest lines, which are saturated, are $\Delta\Omega=0$ transitions ending in $J=1$ and $J=2$. At lower frequency, three intense lines can be assigned to $\Delta\Omega=-1$ transitions ending in $J=0, 1$, and 2 . At the blue side of the spectrum, the intense single line is the $\Delta\Omega=1$ transition to the $J=2$ level. In addition to these six strong features, weak lines have been observed close to the $\Omega=0$ transitions (see inset of Figure 2). Their appearance depends strongly on the alignment of the preparation laser through the supersonic jet. These weak lines can be assigned to transitions arising from the $J=1, \Omega=1, -$ parity level in the $a^3\Pi(v=1)$, which is populated via collisions in the last part of the expansion (after excitation into the $+$ parity level). The splitting observed in the spectrum is (almost) directly the Λ -doublet splitting in the $k^3\Pi_0$ spin-multiplet component, as the contribution of the Λ -doublet splitting in the $a^3\Pi_1$ state is only on the order of 0.01 cm^{-1} .¹⁵ For both the $k^3\Pi_1$ and $k^3\Pi_2$ spin-multiplet components the Λ -doublet splitting is expected to be too small to be resolved.

Transitions can be labelled with $^{\Delta N} \Delta J_{F_{\text{upper}}, F_{\text{lower}}} \times (J_{\text{lower}})$ and the parity of the lower state. For example, the two strongest features in Figure 1 are the $^oQ_{22}(1)$ and the $^pR_{22}(1)$ transitions starting from the $+$ parity (f parity) level. The measured transitions are tabulated in Table I. It is noted that the main error in the transition frequency of the CO lines originates from the determination of the line positions of the Te_2 calibration spectra. The $k^3\Pi(v=0) \leftarrow a^3\Pi(v=1)$ spectrum has also been measured after the preparation of $J=2, \Omega=1, +$ parity level in order to obtain more data for the $v=0$ state. The frequency and the assignment of the eight possible transitions are given in Table II.

Apart from the $v=0$ vibronic band in the $k^3\Pi$ state, the spectra of the $v=1-6$ have been measured as well [after preparation of $a^3\Pi(v=1, J=1, \Omega=1, +$ parity) level]. No lines were found in the region where we expected the $v=7$. The structure of the rotational spectra of these vibrations are similar to that of the $v=0$ spectrum (Figure 2), although for the $v=6$ states only the $\Delta\Omega=0$ transitions could be measured. The spectral region containing transitions to the $v=5$ state is shown in Figure 3. Only transitions to $\Omega=1$ and $\Omega=2$ could be assigned. In the region where the lines to the $\Omega=0$ component are expected, strong lines are visible originating from another electronic state. These lines are tabulated in Table III. These strong lines are narrow and more intense than the $\Omega=1$ transitions of the k state. As the most intense lines of the $k^3\Pi \leftarrow a^3\Pi$ already show effects of saturation, lines can still be stronger if the ionization efficiency from the excited state is higher. Therefore, it is very likely that these extra lines involve transitions to Rydberg states.

For ^{13}CO , the rotational spectra of the $v=0-6$ states have been measured as well. The structure of each spectrum is again similar to that shown in Figure 2. In contrast to

TABLE I. Frequencies (in cm^{-1}) and assignments for the observed $k^3\Pi(v) \leftarrow a^3\Pi(v=1)$ transitions of ^{12}CO . The parity of the lower level is indicated by e/f. The differences between observed and calculated frequencies are also shown.

v	$^oP_{12}(1)$	$^pQ_{12}(1)$	$^eR_{12}(1)$	$^eQ_{22}(1)$	$^fR_{22}(1)$	$^sR_{32}(1)$
0	f 40112.52(08)	-0.03 f 40114.37(08)	f 40119.68(07)	f 40144.92(07)	-0.15 f 40150.07(07)	-0.05 f 40175.49(07)
	e 40111.95(08)	-0.05 e 40114.95(08)	e 40119.21(08)	0.15		
1	f 40923.15(10)	0.08 f 40924.99(10)	f 40930.26(10)	f 40955.83(10)	-0.26 f 40961.12(10)	-0.02 f 40986.95(08)
2	f 41739.34(10)	-0.03 f 41741.23(08)	f 41746.33(07)	f 41771.90(10)	0.11 f 41776.84(10)	0.06 f 41801.96(07)
			e 41745.82(10)	-0.07		
3	f 42561.18(07)	-0.02 f 42562.93(10)	f 42568.07(06)	f 42594.44(10)	-0.12 f 42599.40(10)	-0.06 f 42625.88(07)
4	f 43365.47(08)	0.01 f 43367.17(30)	f 43372.30(10)	f 43398.52(10)	-0.10 f 43403.42(10)	-0.05 f 43429.83(10)
5			f 44250.39(10)	-	f 44255.62(10)	-
6			f 44970.30(20)	0.17 f 44974.45(20)	-0.30	

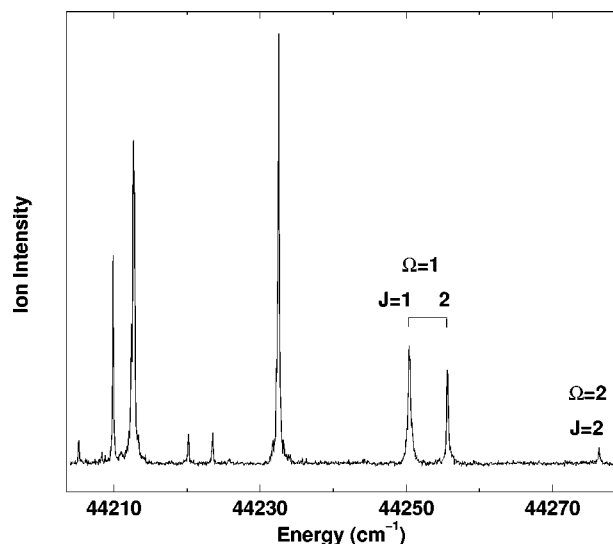


FIG. 3. (1+1)-REMPI spectrum of the spectral region containing the $k^3\Pi$ ($v=5$) $\leftarrow a^3\Pi$ ($v=1, J=1, \Omega=1$) band of ^{12}CO . Only the transitions to the $\Omega=1$ and $\Omega=2$ substates could be identified. In the region of the $\Omega=0$ substate, extra transition are observed belonging to another electronic state. Although we could not identify this state, all transitions should have the $a^3\Pi$ ($v=1, J=1, \Omega=1, +$ parity) level as lower state.

^{12}CO , the spectral region of the $v=5$ band of ^{13}CO shows no additional lines, and all allowed rotational transitions of the $v=5$ were identified. On the other hand, the spectral region containing the $v=6$ band does contain additional lines (tabulated in Table III). Four lines are again very strong and narrow. Nevertheless, all rotational transitions of $v=6$ band could be assigned. Only the $J=0, \Omega=0$ could not be identified since it is overlapped by a strong transition to the $J=2$ level of the $E^1\Pi$ ($v=1$) state. The frequency of all measured transitions of ^{13}CO are given, together with their assignment, in Table IV.

IV. ANALYSIS AND DISCUSSION

In order to compare data of ^{12}CO , ^{13}CO , and data of ^{12}CO from literature and to determine the molecular constants of the $k^3\Pi$ state of CO, term values for all measured transitions are calculated with respect to the bottom of the $X^1\Sigma^+$ ground state potential well. For each transition in Tables I, II, and IV, the term value of the excited level can be calculated by adding the energy of the preparation step, the energy of the level in the $X^1\Sigma^+$ state from where the preparation has been performed (with respect to $J=0$), and the zero-point energy of the $X^1\Sigma^+$ state.

For the transitions listed in Table I, preparation is performed via excitation on the $Q_2(1) a^3\Pi(v=1) \leftarrow X^1\Sigma^+(v=0)$ transition of ^{12}CO which is at $50\,189.20\text{ cm}^{-1}$.¹⁵ The zero-point energy (1081.586 cm^{-1}) and the energy of the $J=1$ level in the $X^1\Sigma^+$ state (3.845 cm^{-1}) has been calculated using the Hamiltonian and molecular constants of Ref. 16. For the transitions originating from the e parity level, the term values should be corrected by subtracting 394 MHz, i.e., the Λ -doubling in the $a^3\Pi(v=1, J=1, \Omega=1)$ state.¹⁵ In the same way, the term values of the $k \leftarrow a$ transitions after

TABLE II. Rotational transitions observed in the $k^3\Pi(v=0)\leftarrow a^3\Pi(v=1)$ band of ^{12}CO after preparation of the $J=2, \Omega=1, +$ parity (e parity) level in the $a^3\Pi(v=1)$ state. The differences between observed and calculated frequencies are also shown. Frequencies are given in cm^{-1} .

$^oP_{12}(2)$	40107.89(05)	0.04	$^pQ_{12}(2)$	40113.17(05)	0.05	$^oR_{12}(2)$	40119.69(10)	0.04
$^pP_{22}(2)$	40138.43(05)	-0.16	$^oQ_{22}(2)$	40143.54(05)	-0.10	$^pR_{22}(2)$	40151.16(05)	-0.05
			$^pR_{32}(2)$	40169.03(05)	0.11	$^sR_{32}(2)$	40177.47(07)	0.08

preparation via the $R_2(1)$ (Table II), at $50\,195.68\text{ cm}^{-1}$,¹⁵ have been calculated. Baker *et al.* have reported rotational transitions of the $k^3\Pi(v=1)\leftarrow X^1\Sigma^+(v=0)$,⁷ and the $k^3\Pi(v=3,4,6)\leftarrow X^1\Sigma^+(v=0)$ bands (note the different vibrational labeling relative to the original papers). From their reported frequencies, term values have been determined by adding the appropriate ground state energies.

For ^{13}CO , the energies in the $X^1\Sigma^+$ state have been calculated with molecular constants obtained via isotopic scaling using the relations:¹⁷

$$\begin{aligned} T_e^i &= T_e, & \omega_e^i &= \omega_e \rho, & \omega_e x_e^i &= \omega_e x_e \rho^2, \\ B_e^i &= B_e \rho^2, & D_e^i &= D_e \rho^4, & \alpha_e^i &= \alpha_e \rho^3, \end{aligned} \quad (1)$$

where

$$\rho = \sqrt{\frac{\mu}{\mu^i}} = 0.977708 \quad (2)$$

with μ and μ^i the reduced masses of ^{12}CO and ^{13}CO . The zero-point energy of ^{13}CO is thus calculated to be 1057.548 cm^{-1} . The frequency of the $Q_2(1) a^3\Pi(v=1)\leftarrow X^1\Sigma^+(v=0)$ transition of ^{13}CO has been determined to be $50\,156.507(7)\text{ cm}^{-1}$ by recording the excitation spectrum (measured with the MCP detector) simultaneously with the iodine absorption spectrum¹⁸ at the fundamental wavelength (597 nm).

The term values of each vibronic state of ^{12}CO and ^{13}CO have been fitted to the roots of the effective $^3\Pi$ Hamiltonian matrix of Field *et al.*¹⁵ to determine the values for the vibrational energy T_v , the rotational constant B_v , the spin-orbit

constant A_v , the parity dependent spin-spin constant C^δ , and the centrifugal constant D_v . The results are presented in Table V. Also listed are the number of transitions from the present study and from Baker *et al.* (in parenthesis) included in the fit. The calculated rotational constant of ^{12}CO obtained via isotopic scaling of the rotational constant of ^{13}CO (B_v/ρ^2), is shown for comparison. The agreement with the measured values is rather good. In Tables I, II, and IV, the value of the difference between observed and calculated frequency is given behind each observed transition.

Some comments have to be made. The observed minus calculated values of several transitions to the $k^3\Pi(v=1)$ state of ^{12}CO are larger than the observed error. For example both the $^oQ_{22}(1)$ and the $^pP_{22}(2)$ transitions, with the same upper level ($J=1, \Omega=1$), are calculated 0.15 cm^{-1} too high. The same level is calculated 0.21 cm^{-1} too high in the $v=0$ of ^{13}CO , and 0.26 cm^{-1} too high in the $v=1$ of ^{12}CO , while this discrepancy can also be observed for the other vibrations of ^{12}CO although less pronounced. This clearly indicates that the k state is perturbed.

While analyzing the data of the $v=3$ of ^{12}CO , there appeared to be a frequency shift between our data and the data of Baker and Launay.⁵ This shift has been included as a parameter in the fit program, resulting in a value of $0.24(3)\text{ cm}^{-1}$ that should be subtracted from the data of Baker and Launay. This shift has not been observed for the other bands. It should be noted that the observed minus calculated values for the transitions reported by Baker *et al.*^{5,7} are within the reported errors for all vibronic bands.

Only three parameters could be determined for the $v=5$ band of ^{12}CO , since only three transitions could be assigned. C^δ has been kept fixed. Its actual value has only a minor influence on the other constants. An extra parameter had to be included to obtain a reasonable fit for the $v=5$ band of ^{13}CO . There appears to be a shift in one of the Ω ladders: either one has to subtract $1.82(4)\text{ cm}^{-1}$ from the $\Omega=0$ transitions, or add $0.91(2)\text{ cm}^{-1}$ to the $\Omega=1$ transitions, or subtract $1.82(4)\text{ cm}^{-1}$ from the $\Omega=2$ transitions. The value of the spin-orbit constant A_5 is therefore an averaged value with a large uncertainty. Note that this effect is not observed for the $v=5$ of ^{12}CO since we could not identify the $\Omega=0$ levels.

No transitions of the $k^3\Pi$ state have been observed in the region of the $v=7$. By electron impact spectroscopy, Mazeau *et al.*¹ observed the $v=4-8$ followed by a ‘‘plateau.’’ The $v=7$ and $v=8$ were broadened, which has been explained by partial predissociation of these levels. Higher levels are completely predissociated, leading to a dissociation continuum (the ‘‘plateau’’). These predissociation phenomena were attributed to an avoided crossing of the $k^3\Pi$

TABLE III. Additional rotational transitions observed in the region of $k^3\Pi(v)\leftarrow a^3\Pi(v=1)$ bands of ^{12}CO and ^{13}CO . The label v is only given to indicate in which region of the $k^3\Pi$ state the transition is found. All frequencies are in cm^{-1} . This list is not complete, since only small spectral regions around the $k^3\Pi\leftarrow a^3\Pi(v=1)$ bands have been investigated. The transitions in ^{12}CO are shown in Figure 3. Two strong and narrow lines of ^{13}CO can be assigned as transitions to the $E^1\Pi(v=1)$ Rydberg state (Ref. 10). Although we were not able to assign the other transitions, they all have the $a^3\Pi(v=1, J=1, \Omega=1)$ level as lower state.

^{12}CO				^{13}CO
v	extra line	v	extra line	
5	44 205.24(10)	6	44 701.8(5)	weak, narrow
5	44 209.93(10)	6	44 794.1(2.0)	weak, broad ($\sim 15\text{ cm}^{-1}$)
5	44 212.66(10)	6	44 879.36(8)	$E^1\Pi(v=1, J=1)$
5	44 220.13(08)	6	44 886.90(7)	$E^1\Pi(v=1, J=2)$
5	44 223.51(08)	6	45 067.7(5)	strong, narrow
5	44 232.53(10)	6	45 080.1(5)	strong, narrow
		6	45 093.1(5)	weak, narrow

TABLE IV. Frequencies (in cm^{-1}) and assignments for the observed $k^3\Pi(v) \leftarrow a^3\Pi(v=1)$ transitions of ^{13}CO . The parity of the lower level is indicated by e/f. The differences between observed and calculated frequencies are also shown.

v	$^oP_{12}(1)$	$^oP_{12}(1)$	$^oQ_{12}(1)$	$^oQ_{12}(1)$	$^oQ_{22}(1)$	$^oQ_{22}(1)$	$^oR_{22}(1)$	$^oR_{22}(1)$	$^oR_{32}(1)$	$^oR_{32}(1)$								
0	f	40160.08(08)	0.01	f	40161.74(08)	0.02	f	40166.90(08)	0.05	f	40192.17(10)	-0.21	f	40197.13(10)	-0.10	f	40222.71(08)	0.10
	e	40159.45(09)	-0.02	e	40162.33(10)	-0.01	e	40166.29(08)	0.03									
1	f	40952.40(08)	0.01	f	40954.13(08)	-0.02	f	40959.24(08)	-0.02	f	40985.19(30)	-0.05	f	40990.08(30)	-0.07	f	41015.96(05)	0.00
	e	40951.86(08)	-0.01	e	40954.69(08)	0.00	e	40958.77(08)	0.03									
2	f	41750.88(10)	-0.09	f	41752.70(07)	0.01	f	41757.70(07)	-0.03	f	41783.64(10)	0.07	f	41788.36(10)	-0.04	f	41814.07(05)	0.00
	e	41750.40(10)	-0.05	e	41753.30(07)	0.07	e	41757.24(10)	0.03									
3	f	42554.40(07)	-0.02	f	42555.96(10)	0.01	f	42560.92(05)	0.01	f	42587.59(07)	0.01	f	42592.17(07)	-0.03	f	42618.80(07)	0.01
	f	43342.14(15)	-0.02	f	43343.87(15)	0.01	f	43348.76(15)	0.03	f	43375.22(10)	-0.01	f	43379.90(10)	-0.01	f	43406.50(50)	0.26
5	f	44189.01(05)	0.00	f	44191.16(05)	0.01	f	44196.22(05)	0.00	f	44214.62(06)	0.01	f	44219.82(08)	-0.02	f	44239.64(06)	0.00
	e	44188.72(08)	-0.04	e	44191.42(05)	0.00												
6				f	44889.02(07)	-0.01	f	44893.56(07)	-0.01	f	44920.33(10)	0.07	f	44924.63(10)	0.02	f	44951.15(07)	-0.02

state with a dissociative state. Apparently, the lifetime of the $v=7$ level is already sufficiently short (sub-ns) that it escapes efficient detection in the employed REMPI scheme.

Figure 4 is a graphical representation of the molecular constants. Shown are the rotational constants B_v , the spin-orbit constants A_v , and the differences $\Delta T_{v+1/2} = T_{v+1} - T_v$ as a function of the vibrational quantum number v for both ^{12}CO and ^{13}CO . It is immediately seen that the behavior of each constant is the same for both isotopomers. Furthermore, if there were no perturbations, all curves would be a smooth function of v . This is certainly not the case. Even the most regular part, the lowest three vibrations, immediately show the presence of a perturbation since the vibrational spacing *increases*. These observations suggest that the strongest perturbation is caused by another $^3\Pi$ state. The $c^3\Pi$ state might be a good candidate, as has already been suggested by Mazeau *et al.*¹ The $c^3\Pi(v=0)$ of ^{12}CO is at $93\,158.5\text{ cm}^{-1}$,¹⁹ close to the $v=2$ of the $k^3\Pi$ state (at $93\,042.4\text{ cm}^{-1}$), and shows strong perturbations in the rotationally resolved spectrum.^{9,20,21} The $v=1$ of the $c^3\Pi$ state has only been observed by Mazeau *et al.*¹ with electron impact spectroscopy, and is at $95\,361(80)\text{ cm}^{-1}$, close to the $v=5$ of the $k^3\Pi$ state.

In order to be sure about the vibrational labeling, or in other words that the state labeled $v=0$ here is really the lowest vibronic state, we have performed a global fit of all term values of $v=0-3$ of ^{12}CO and ^{13}CO , using the aforementioned $^3\Pi$ Hamiltonian, the isotopic scaling relations of Eq. (1), and the usual vibrational spectroscopic relations. The vibrational dependence of the spin-orbit constant is, in analogy with the rotational constant, given by $A_v = A_e - \gamma_e(v + 1/2)$. Furthermore, the spin-orbit constant is assumed to be equal for both isotopomers. The parity dependent spin-spin parameter C^δ is assumed to be independent of the vibrational state, and is equal for both isotopomers. The data of Baker *et al.* has not been included in the fit, in order to have the same set of rotational levels for each vibronic state. The result is a fit of 69 term values with a standard deviation of 0.35 cm^{-1} , which is of course worse than the individual fits shown in Table V due to perturbations. The molecular constants of the $k^3\Pi$ state of CO are: $T_e = 91\,012.2(2)\text{ cm}^{-1}$, $\omega_e = 805.1(2)\text{ cm}^{-1}$, $\omega_e x_e = -2.85(6)\text{ cm}^{-1}$, $B_e = 1.29(3)\text{ cm}^{-1}$, $A_e = 29.9(1)\text{ cm}^{-1}$, $\gamma_e = -0.28(5)\text{ cm}^{-1}$, and $C^\delta = 0.27(7)\text{ cm}^{-1}$. The constant α_e could not be determined. To verify the vibrational assignment, suppose now that the vibrational labeling should be raised by one. Fitting the same data set leads then to a standard deviation of 8 cm^{-1} , thus confirming our present assignment.

V. CONCLUSION

A new vibronic band of the $k^3\Pi$ state has been observed for ^{12}CO . This band is at lower frequency than the vibrational origin which is reported in literature,^{5,7,8} implying that the vibrational numbering should be corrected. The new vibronic band has been assigned as the $v=0$ state. The rotationally resolved spectra of $k^3\Pi(v=0-6) \leftarrow a^3\Pi(v=1)$ bands have been measured via (1+1)-REMPI of a molecular

TABLE V. Molecular constants for the $k^3\Pi(v=0-6)$ states of ^{12}CO and ^{13}CO . All values are in cm^{-1} . N is the number of transitions in the fit. Note that T_v is taken with respect to the potential minimum of the $X^1\Sigma^+$ ground state and includes a zero-point energy of 1081.586 cm^{-1} for ^{12}CO and 1057.548 cm^{-1} for ^{13}CO .

Molecular constants of ^{12}CO						
v	T_v	B_v	A_v	C_v^δ	D_v	N
0	91 415.62(07)	1.285(08)	30.02(04)	0.28(4)	-	17
1	92 226.66(07)	1.284(05)	30.46(05)	0.29(6)	$4.6(3.0) \cdot 10^{-5}$	6+(7)
2	93 042.40(10)	1.269(16)	29.91(04)	0.24(4)	-	7
3	93 865.26(03)	1.244(01)	30.97(01)	0.30(2)	$1.0(1) \cdot 10^{-5}$	6+(103)
4	94 669.37(05)	1.230(01)	30.80(03)	0.30(3)	$1.7(2) \cdot 10^{-5}$	6+(40)
5	95 520.71(22)	1.344(40)	25.32(12)	-	-	3
6	96 241.09(10)	1.168(20)	31.29(15)	0.25(4)	$2.5(4) \cdot 10^{-5}$	2+(16)
Molecular constants of ^{13}CO						
v	T_v	B_v	A_v	C_v^δ	B_v/ρ^2	N
0	91 406.22(10)	1.231(20)	29.95(05)	0.30(5)	1.288(20)	9
1	92 199.04(02)	1.247(04)	30.43(01)	0.27(1)	1.304(04)	9
2	92 997.44(05)	1.225(12)	30.23(03)	0.27(3)	1.281(12)	9
3	93 801.63(04)	1.170(07)	30.97(02)	0.32(3)	1.223(07)	6
4	94 589.22(07)	1.188(15)	30.76(06)	0.25(4)	1.242(15)	6
5	95 428.30(40)	1.354(10)	23.6(1.0)	0.13(2)	1.416(10)	8
6	96 134.54(15)	1.100(30)	30.70(04)	0.23(6)	1.150(30)	5

beam of metastable ^{12}CO or ^{13}CO molecules in a single quantum state, being the $a^3\Pi(v=1, J=1, \Omega=1)$ state. The spectrum of the $v=5$ state of ^{12}CO and the spectra of ^{13}CO have been observed for the first time. For each vibronic state of ^{12}CO and ^{13}CO , the rotational transitions were assigned and the term values were fitted to the effective $^3\Pi$ Hamiltonian of Field *et al.*,¹⁵ providing the molecular constants of

each level. Additional lines, belonging to transitions into another electronic state, have been observed near the $v=5$ of ^{12}CO and the $v=6$ of ^{13}CO . Comparison of the molecular constants of all bands confirms the vibrational assignment and shows that the $k^3\Pi$ state is strongly perturbed. However, these perturbations seem to be the same for both isotopomers, suggesting that the (strongest) perturbations are caused by another $^3\Pi$ state.

It is known that the $k^3\Pi$ state causes local perturbations, leading to accidental predissociations, in the $E^1\Pi(v=0,1)$ states.^{4,5,7,10} The majority of perturbations were found at high J levels (up to 50). Since most of our molecular constants were derived from $J=0, 1$, and 2 levels (for some vibronic bands of ^{12}CO data from Baker *et al.* was included), no precise information could be obtained for these local perturbations. However, in the present study detailed information has been obtained about the exact position of the $k^3\Pi$ vibronic states in the $90\,000$ – $100\,000\text{ cm}^{-1}$ energy range, where many other electronic states have been observed.

ACKNOWLEDGMENTS

This work is part of the research program of the ‘‘Stichting voor Fundamenteel Onderzoek der Materie (FOM),’’ which is financially supported by the ‘‘Nederlandse Organisatie voor Wetenschappelijk Onderzoek (NWO),’’ and receives direct support by NWO via PIONIER-Grant No. 030-66-89.

¹J. Mazeau, C. Schermann, and G. Joyez, *J. Electron Spectrosc. Relat. Phenom.* **7**, 269 (1975).

²S.V. O’Neil and H.F. Schaefer III, *J. Chem. Phys.* **53**, 3994 (1970).

³B.N. Wan and H. Langhoff, *Z. Phys. D* **21**, 245 (1991).

⁴J. Baker, J.L. Lemaire, S. Couris, A. Vient, D. Malmasson, and F. Rostas, *Chem. Phys.* **178**, 569 (1993).

⁵J. Baker and F. Launay, *J. Mol. Spectrosc.* **165**, 75 (1994).

⁶J. Baker, W.-Ü.L. Tchang-Brillet, and P.S. Julienne, *J. Chem. Phys.* **102**, 3956 (1995).

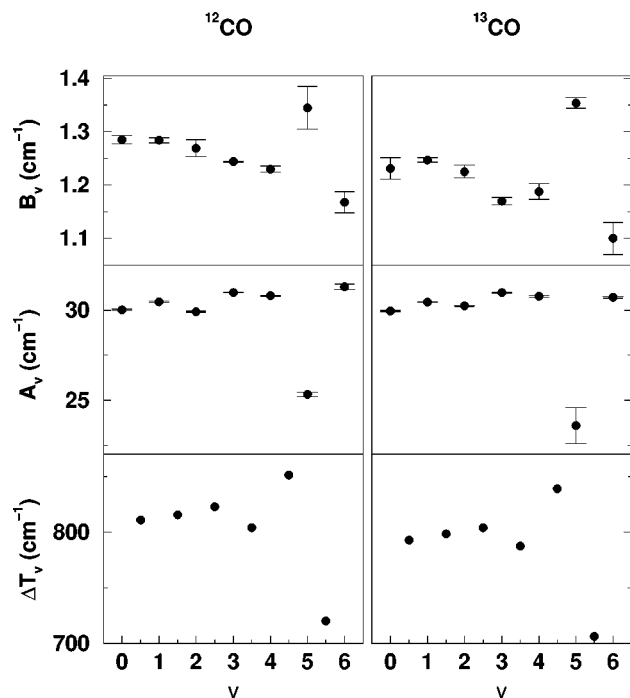


FIG. 4. Graphical representation of the molecular constants of ^{12}CO and ^{13}CO as a function of the vibrational quantum number v . Shown are the rotational constant B_v , the spin-orbit constant A_v , and the vibrational spacing $\Delta T_{v+1/2} = T_{v+1} - T_v$.

- ⁷J. Baker, *J. Mol. Spectrosc.* **167**, 323 (1994).
- ⁸A. Mellinger and C.R. Vidal, *J. Chem. Phys.* **101**, 104 (1994).
- ⁹I. Dabrowski, M. Vervloet, and D.-C. Wang, *Can. J. Phys.* **65**, 1171 (1987).
- ¹⁰P. Cacciani, W. Hogervorst, and W. Ubachs, *J. Chem. Phys.* **102**, 8308 (1995).
- ¹¹R.T. Jongma, M.G.H. Boogaarts, and G. Meijer, *J. Mol. Spectrosc.* **165**, 303 (1994).
- ¹²R.T. Jongma, G. Berden, and G. Meijer, *J. Chem. Phys.* **107**, 7034 (1997).
- ¹³W.C. Wiley and I.H. McLaren, *Rev. Sci. Instrum.* **26**, 1150 (1955).
- ¹⁴J. Cariou and P. Luc, *Atlas du Spectre d'absorption de la Molecule de Tellure* (CNRS, Orsay, France, 1980).
- ¹⁵R.W. Field, S.G. Tilford, R.A. Howard, and J.D. Simons, *J. Mol. Spectrosc.* **44**, 347 (1972).
- ¹⁶A.W. Mantz, J.-P. Maillard, W.B. Roh, and K.N. Narahari Rao, *J. Mol. Spectrosc.* **57**, 155 (1975).
- ¹⁷G. Herzberg, *Molecular Spectra and Molecular Structure, Vol. I: Spectra of Diatomic Molecules* (Van Nostrand, New York, 1950).
- ¹⁸S. Gerstenkorn and P. Luc, *Atlas du Spectroscopie d'absorption de la Molecule d'iode* (CNRS, Paris, 1978) S. Gerstenkorn and P. Luc, *Rev. Phys. Appl.* **14**, 791 (1979).
- ¹⁹S.G. Tilford, *J. Chem. Phys.* **50**, 3126 (1969).
- ²⁰T. Rytel and M. Rytel, *Acta Phys. Hung.* **55**, 69 (1984).
- ²¹T. Rytel and M. Rytel, *Acta Phys. Hung.* **59**, 355 (1986).